PRECISE 3D REACTOR CORE CALCULATION USING SPHERICAL HARMONICS AND DISCONTINUOUS GALERKIN FINITE ELEMENT METHODS

INTERNATIONAL CONFERENCE ON PHYSICS OF REACTORS 2022
PHYSOR 2022 • PITTSBURGH, PA, MAY 15-20, 2022
doi.org/10.13182/PHYSOR22-37354

Kenneth Assogba
Université Paris-Saclay, CEA, Service d'Études
des Réacteurs et de Mathématiques Appliquées
91191 Gif-sur-Yvette, France
&
CMAP, École Polytechnique
Institut Polytechnique de Paris
91128 Palaiseau, France
kenneth.assogba@cea.fr

Lahbib Bourhrara
Université Paris-Saclay, CEA, Service d'Études
des Réacteurs et de Mathématiques Appliquées
91191 Gif-sur-Yvette, France
lahbib.bourhrara@cea.fr

Igor Zmijarevic
Université Paris-Saclay, CEA, Service d'Études
des Réacteurs et de Mathématiques Appliquées
91191 Gif-sur-Yvette, France
igor.zmijarevic@cea.fr

Grégoire Allaire
CMAP, École Polytechnique
Institut Polytechnique de Paris
91128 Palaiseau, France
gregoire.allaire@polytechnique.fr

ABSTRACT

We study the use of P_N method in angle and Discontinuous Galerkin in space to solve 3D neutron transport problem. P_N method consists in developing the angular flux on truncated spherical harmonics basis. In this paper, we couple this method with the discontinuous finite elements in space to obtain a complete discretisation of the multigroup neutron transport equation. To investigate its precision, the method was applied to Takeda and C5G7 benchmark problems. These calculations point out that the proposed P_N-DG method is capable of producing accurate solutions in small computational time, and that it is able to handle complex 3D geometries.

Keywords PN method · DG FEM · Discontinuous finite element method · neutron transport equation

1 Introduction

Based on the variational formulation proposed in [1], a new approximation method for the Boltzmann transport equation is presented in [2]. The objective of this study is to present the results obtained with this approach applied to nuclear reactor core calculations in three-dimensional geometries.

The first step of approximation consists in expanding the angular flux on spherical harmonics basis and in truncating the development to the order N: that is the P_N method. In the literature we find transport solvers based on this method, for example EVENT [3] and VARIANT [4]. This method is associated with discontinuous finite element method in space to provide a complete discretisation of the Boltzmann transport equation. The proposed numerical method can treat 2D unstructured, non-conforming and curved meshes, and 3D prismatic meshes. Hence heterogeneous pin-cell geometries with concentric annular regions can be modeled without any approximation. Time-consuming operations

like matrix-vector multiplications are parallelized using OpenMP. All the developments are made in the transport solver NYMO [2] in the scope of CEA platform APOLLO3 ® [5].

In the next section, we describe the numerical approximation. Then, we present solutions to Takeda [6] and 3-D C5G7 MOx fuel assembly [7] benchmark problems.

2 P_N-DG angular-space discretisation

We describe the approximation proposed to the monoenergetic transport source problem. Generalization to the multigroup problem is straightforward. The details of the discretization is given in [2].

2.1 Continuous Problem

Let D, the reactor domain, be an open bounded domain in $\mathbf{R}^3$, of boundary ∂D and outward normal n. $\mathbf{S}^2$ the unit sphere of $\mathbf{R}^3$. We consider the within group transport source equation:

$$\begin{cases} \omega \cdot \nabla u + \sigma u = q & \text{in } X = D \times \mathbf{S}^2 \\ u = f & \text{on } \Gamma_- \end{cases} \tag{1}$$

with f the incoming flux, q the source term, σ the total cross section assumed to be a positive non-vanishing function and $\Gamma_\pm = \{(x,\omega) \in \partial D \times \mathbf{S}^2,\ \pm\omega \cdot n(x) > 0\}$. Let v be a smooth test function, we multiply (1) by $(v + \frac{1}{\sigma}\omega \cdot \nabla v)$ and integrating over the phase space $X = D \times \mathbf{S}^2$,

$$\int_X \left(\frac{1}{\sigma}(\omega \cdot \nabla u)(\omega \cdot \nabla v) + \sigma u v \right) + \int_X \left(u(\omega \cdot \nabla v) + (\omega \cdot \nabla u) v \right) = \int_X q \left(v + \frac{1}{\sigma}(\omega \cdot \nabla v) \right).$$

After using Green's formula, we obtain the variational problem,

$$\text{find } u \in W \ \text{ such that } \ a(u,v) = L(v), \ \ \forall v \in W \tag{2}$$

with

$$\begin{aligned} W &= \left\{ v \in L^2(X) \ / \ \omega \cdot \nabla v \in L^2(X),\ v|_{\Gamma_+} \in L^2(\Gamma_+, |\omega \cdot n| ds d\omega) \right\}, \\ a(u,v) &= \int_X \left(\frac{1}{\sigma}(\omega \cdot \nabla u)(\omega \cdot \nabla v) + \sigma u v \right) + \int_{\Gamma_+} uv(\omega \cdot n), \\ L(v) &= \int_X q \left(v + \frac{1}{\sigma}(\omega \cdot \nabla v) \right) - \int_{\Gamma_-} f v (\omega \cdot n). \end{aligned}$$

Under reasonable assumptions about data, it has been established in [1] that the variational formulation (2) is equivalent to the original transport problem (1).

2.2 Angular Flux Approximation

The P_N method consists in truncating the expansion of the flux $u(x,\omega)$ on the real-valued spherical harmonics $y_n^m(\omega)$ (see [8]) to the order N, that is:

$$u(x,\omega) = \sum_{n=0}^{N} \sum_{m=-n}^{n} u_n^m(x) y_n^m(\omega),$$

the components $u_n^m(x)$ of the flux are called angular flux moments, with the scalar flux and current given by $u_0^0(x)$ and $u_1^m(x)$ respectively.

Next, let D_h be a subdivision of D into distinct regions D_r, such that,

$$D = \bigcup_{D_r \in D_h} D_r.$$

On each region D_r, we assume the flux moment is a polynomial, that is $u_n^m \in Q_k$. Where Q_k is the space of d-variate polynomials of degree k:

$$Q_k = \text{span} \left\{ x^{\alpha_1} y^{\alpha_2} z^{\alpha_3} \ / \ 0 \le \sum_{i=1}^{3} \alpha_i \le k \right\}.$$

In 3D, $\dim Q_k = \binom{k+3}{3} = \frac{(k+3)!}{3!k!}$, in particular $\dim Q_0 = 1$, $\dim Q_1 = 4$ and $\dim Q_2 = 10$. Once the basis of Q_k is fixed, the coefficients $u_{n,j}^m$ fully determine the approximated flux:

$$u(x,\omega) = \sum_{n=0}^{N} \sum_{m=-n}^{n} \sum_{j=1}^{J} u_{n,j}^m \varphi_j(x) y_n^m(\omega), \tag{3}$$

where $(\varphi_j(x))_{j=1,\cdots,J}$ is a basis of Q_k. We approximate the incoming flux f and the source term q in the same way. In each region D_r the number of degrees of freedom is $N^\star = \binom{k+3}{3}(N+1)^2$.

The discrete problem consists in solving in each region D_r the following problem:

$$\text{find } u \in W_h \text{ such that } a(u,v) = L(v), \quad \forall v \in W_h \tag{4}$$

where

$$a(u,v) = \int_{X_r} \left(\frac{1}{\sigma}(\omega \cdot \nabla u)(\omega \cdot \nabla v) + \sigma uv \right) + \sum_{F \in \partial D_r} \int_{F \times \mathbf{S}_+^2} uv(\omega \cdot n),$$

$$L(v) = \int_{X_r} q \left(v + \frac{1}{\sigma}(\omega \cdot \nabla v) \right) - \sum_{F \in \partial D_r} \int_{F \times \mathbf{S}_-^2} \tilde{f} v(\omega \cdot n),$$

$W_h = \operatorname{span}(\varphi_j y_n^m)$ is the local approximation space, $X_r = D_r \times \mathbf{S}^2$, and $\tilde{f} = f$ if we are on the domain boundary ∂D else $\tilde{f}$ is the flux in the adjacent region if the face F is an interface (upwind).

By replacing u with (3) and v with $\varphi_{j'}(x) y_{n'}^{m'}(\omega)$ in (4), we obtain a matrix system of unknowns $u_{n,j}^m$. The determination of these matrices therefore involves the calculation of volume integrals and surface integrals. In three dimensions, each region is given as a base face S extruded along the z direction:

$$D_r = S \times [z_0, z_1].$$

Each face F of ∂D_r is either a horizontal face or a lateral face. The vertical faces are obtained by extruding a line segment, circle or a circular arc in the horizontal plane along the z axis:

$$F = s \times [z_0, z_1].$$

Thus, any 3D calculation comes down to a 2D calculation, which is described in [2].

3 Applications

The numerical method described in section 2 was applied to two 3D core calculation problems available in the literature. The first one is Takeda benchmark [6] and the second is the C5G7 benchmark [7]. These problems provide different configurations (10+3 in total), which offer a wide variety of geometries (cartesian, hexagonal, unstructured) with different optical properties, representative of FBR and PWR reactors. All calculations are performed on a 24 core (48 thread) Intel® Xeon® Silver 4214 CPU at 2.20GHz.

3.1 Takeda Benchmark

The Takeda benchmark [6] comprises four different reactor models with two or three distinct cases per model, this amounts to 10 cases in total. All the calculations were performed using NYMO solver with P_4 order in angle and linear polynomial in space. In all calculated models, the relative errors compared to reference eigenvalue are below 40 pcm, with in particular 1 pcm obtained for case 2 of model 2. We also changed the P_N order to show the asymptotic behaviour of k_{eff} with model refinement (Fig. 3). We present here the results obtained for problems 3 and 4, these being the most heterogeneous and time-consuming. The reference solutions are taken from [6, p. 23].

3.1.1 Takeda model 3: cartesian geometry axially heterogeneous FBR

This model problem (Fig. 1) is a Fast Breeder Reactor (FBR) core that has reflector and internal blanket region. There are three different cases depending on the material inserted in the control rod positions (rods or blanket cells). The core has 1/4 radial and 1/2 axial symmetry and the mesh elements used are of size $\Delta x = \Delta y = \Delta z = 5$ cm. We observe in Table 1 that the error is quite small (less than 38 pcm) with less than 1 min calculation time.

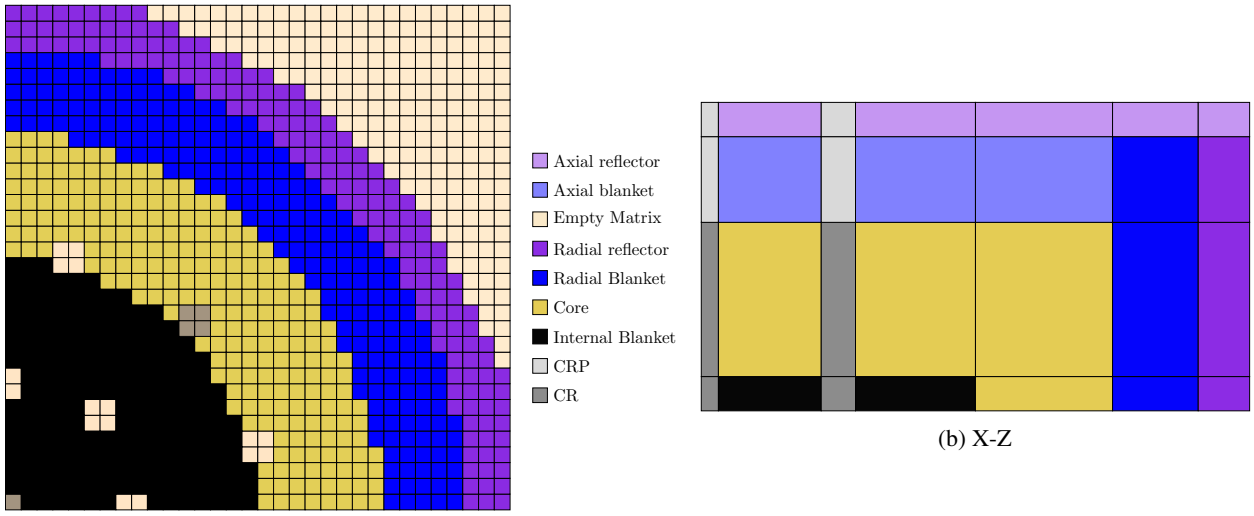

(a) X-Y

(b) X-Z

Figure 1: Takeda model 3.

3.1.2 Takeda model 4: hexagonal geometry small FBR

This model (Fig. 2) is a FBR core and has prismatic hexagonal geometry. Three cases with different control rod patterns are studied: withdrawn (case 1), half inserted (case 2) and fully inserted rods (case 3). For the mesh, all hexagons are divided into 24 (case 1) or 54 (case 2 and 3) equilateral triangles with $\Delta z = 5$ cm. Indeed, the presence of the control rods creates a discontinuity, and the mesh has been refined to take it into account. Table 1 shows that this allows us to obtain excellent results (less than 22 pcm) for all cases. Fig. 3 shows the monotone convergence in angle, especially if we isolate odd and even orders. We go further into the convergence study in section 3.2.

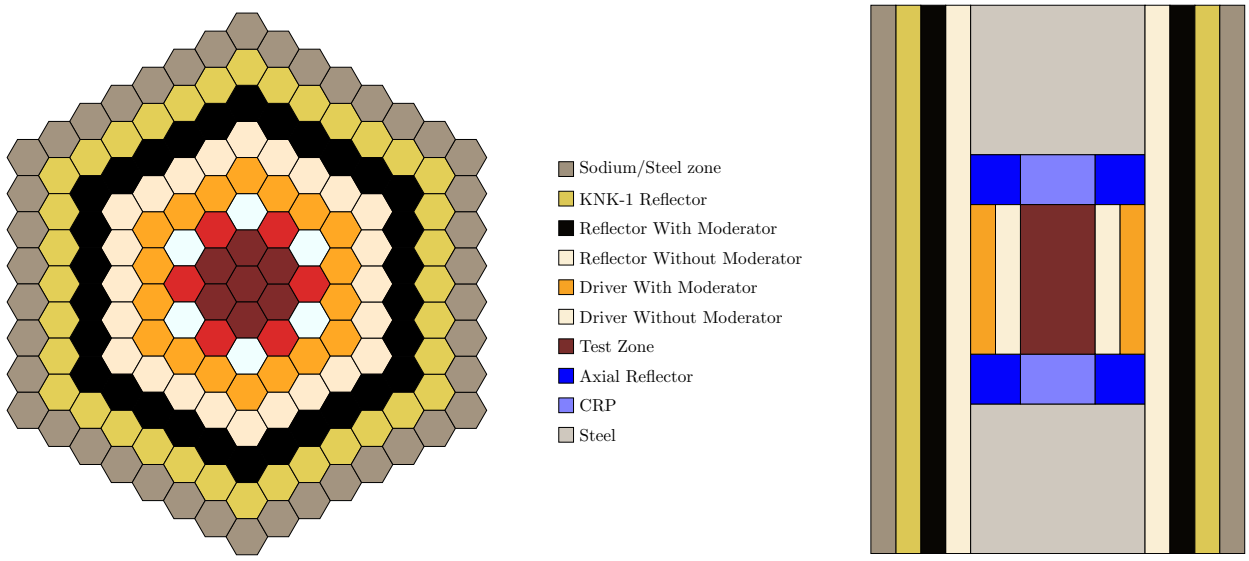

(a) X-Y

(b) X-Z

Figure 2: Takeda model 4.

3.2 Three-dimensional C5G7 Problem

The 3-D extended C5G7 MOx fuel assembly benchmark [7] is a problem designed to evaluate the ability of deterministic transport codes to handle reactor problems without spatial homogenization. It should be noted that in this benchmark,

Table 1: Relative error (in pcm) and computing time (s) obtained with P_4 and linear polynomials for Takeda benchmark models 3 and 4. For model 4, Case 1 comprises 24 equilateral triangles per hexagon while Cases 2 and 3 are refined to 54 triangles.

	Reference	NYMO	error	cpu time
Case 1	0.97090	0.97060	-30	49
Case 2	1.00050	1.00089	38	49
Case 3	1.02140	1.02147	6	51

(a) Model 3

	Reference	NYMO	error	cpu time
Case 1	1.09510	1.09521	10	474
Case 2	0.98330	0.98352	22	2636
Case 3	0.87990	0.87994	4	2349

(b) Model 4

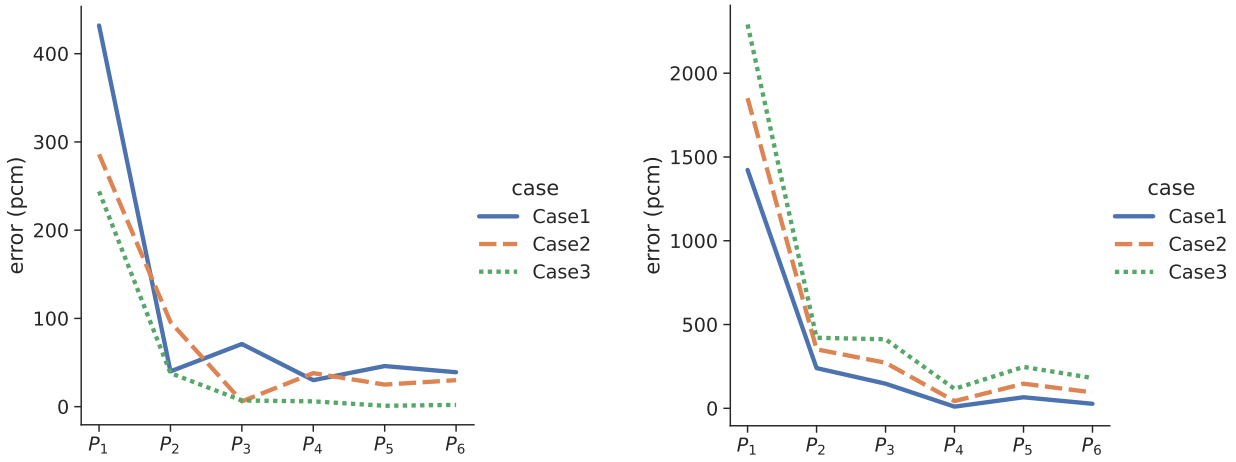

(a) Model 3

(b) Model 4

Figure 3: Evolution of the eigenvalue relative error (in absolute value) according to the angular discretization order.

the cladding surrounding the fuel rod is smeared with the fuel pellet. The objectives are to calculate the effective multiplication factor and the normalized fission rate distributions (pin power) in three axial slices of the core.

3.2.1 Benchmark description and space-angular discretisation

Fig. 4a shows the radial configuration of this 128.52×128.52×128.52 cm^3 small Pressurized Water Reactor (PWR) core, made up of four by four fuel assemblies, modeled in 1/4 radial symmetry and surrounded by a water reflector. Each assembly consists of a 17×17 lattice of square pin cells with the cell side equal to 1.26 cm. Fuel pins, control rods, guide tubes, and fission chambers are of circular shape with a 0.54 cm radius. The reflection boundary condition in zmin plane with inserted control rods makes the problem non-physical, which is explicitly stated in the problem description. Three problems (Unrodded, Rodded A and Rodded B) are considered to correspond to various levels of control rod insertion. The seven-group cross-sections with isotropic scattering for each material and detailed description are provided in [7].

For all calculation, the radial mesh used is described in Fig. 4b. This radial mesh is the unique one applied to all calculations. Axial mesh has been varied starting from the coarsest one (denoted as Z_1) that has only one mesh interval within each fuel slice and reflector, and refining it progressively by subdividing these slices into two (Z_2), four (Z_4) and eight (Z_8) intervals. For polynomial discretisation space, Q_k refers to piecewise polynomial functions space of degree at most k. That is, Q_0 the space of piecewise constant polynomial, Q_1 refers to space of piecewise linear polynomial and Q_2 refers to space of piecewise quadratic polynomial. The eigenvalue calculation is converged when for two successive iterations, the relative variation is less than 10^{-6}.

We performed a series of calculations by varying the P_N order from 1 to 6, the polynomial basis used are constant, linear and quadratic and the axial mesh refinement are 1, 2, 4 or 8. This involves 72 eigenvalue calculations for each test case. As before, each case was run on 24-core computer with an approximate run time between 10s (P_1, Q_0 without axial refinement) and 20h (P_6, Q_2, Z_8) for the most refined case.

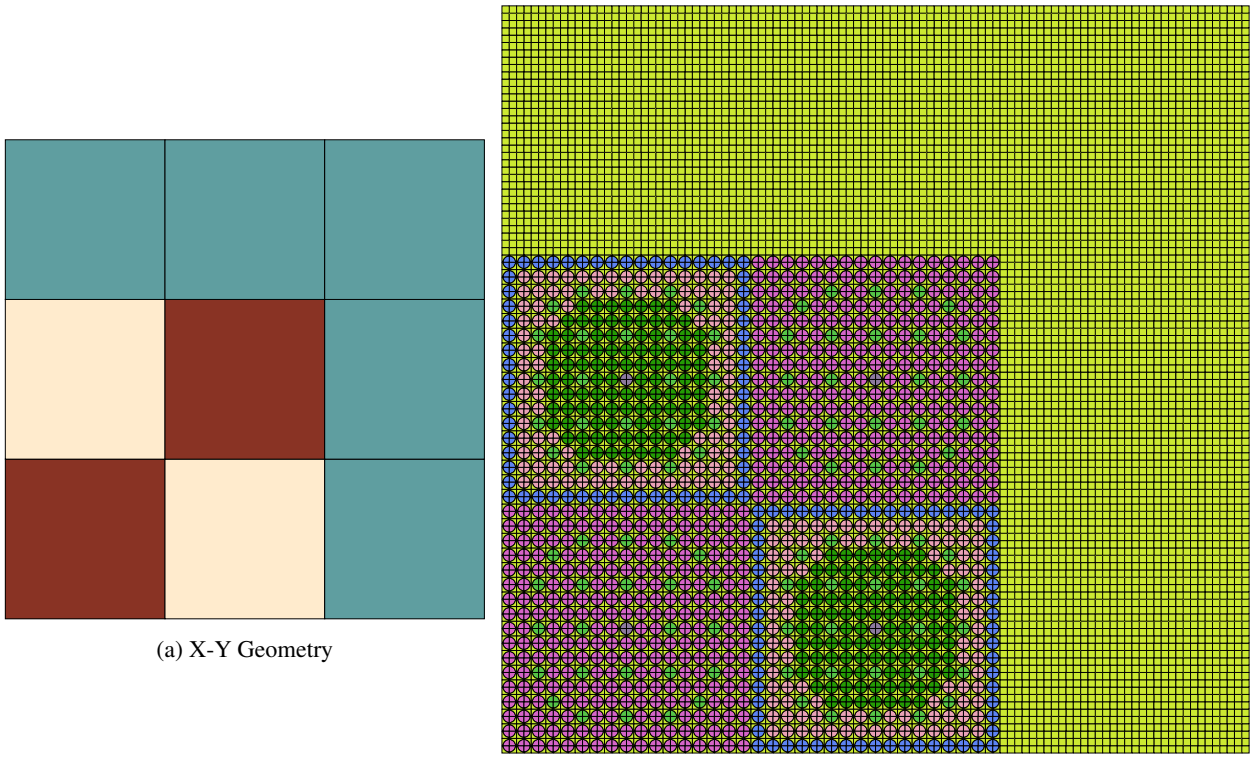

(a) X-Y Geometry

(b) Radial mesh used for calculations.

Figure 4: C5G7 Reactor with UOx (brown), MOx (beige) and reflector (turquoise).

3.2.2 Results of calculation and discussion

The first results show that, for all P_N orders, the error on the Q_0 polynomial space is high, so we discard these configurations from the further analysis. Moreover, the axial refinement does not seem to significantly improve the results. The differences between Z_4 and Z_8 refinements being very small (between 0 and 4 pcm) we excluded Z_8 from the rest of the analysis. Thus, we may conclude that the flux does not vary much axially and that it is not necessary to refine the mesh in this direction. This assumption is partially confirmed by [9], who studied the influence of the control rods by analysing the scalar fluxes along control rods. The authors observe that the axial scalar fluxes decreases in the vicinity of the reflector, but vary little in each slice in MOx and UOx outer assemblies. Moreover, the flux variation is more pronounced in the UOx inner assembly when the control rods are inserted (Rodded A and B). In our case, for Rodded A, the best results are still obtained without refinement, while Rodded B gives better results by subdividing each z-slice in two. For the Unrodded and Rodded A cases, the best results are respectively 12 pcm and -29 pcm and obtained with $P_5\ Q_2\ Z_1$, while for Rodded B the best solution have 6 pcm error and obtained with $P_6\ Q_1\ Z_2$. Considering only the configurations running in less than 3 min (180s) the best result is -48 pcm ($P_1\ Q_2\ Z_1$) for Unrodded, -80 pcm for Rodded A and -162 pcm Rodded B (the two with $P_2\ Q_1\ Z_1$).

Fig. 5 shows the variation of eigenvalue relative error according to P_N order for each of the polynomial spaces Q_1 and Q_2. In all three cases, the results are presented for Z_2 refinement. We make several observations here. First, for all polynomial spaces, separating the even (green lines) and odd (red lines) P_N orders, we observe a monotone convergence. In the first two cases however, the even P_N orders stagnate or increase slightly. This behaviour is for the moment unexplained. Second, for even (resp. odd) P_N the error obtained is smaller in polynomial space Q_1 (resp. Q_2). And finally, we note that the even (resp. odd) P_N converge to the reference solution by overestimating (resp. underestimating) it. This oscillatory approach to the asymptotic regime, but monotonous if one takes separately odd and even orders, has already been observed in previous works on the 2D solutions, in [2] on reactivity and in [10] on the flux shape. In the latter, a different finite element approximation is used, which may suggest that this behavior is due to the properties of spherical harmonic approximation itself, but for the moment it remains unexplained. All these observations deserve further investigation.

We next proceed to the pin power calculations with the configurations that provide the best multiplication factor of each case. Table 2 shows the error made on maximum pin power, the average (AVG), root mean square (RMS) and

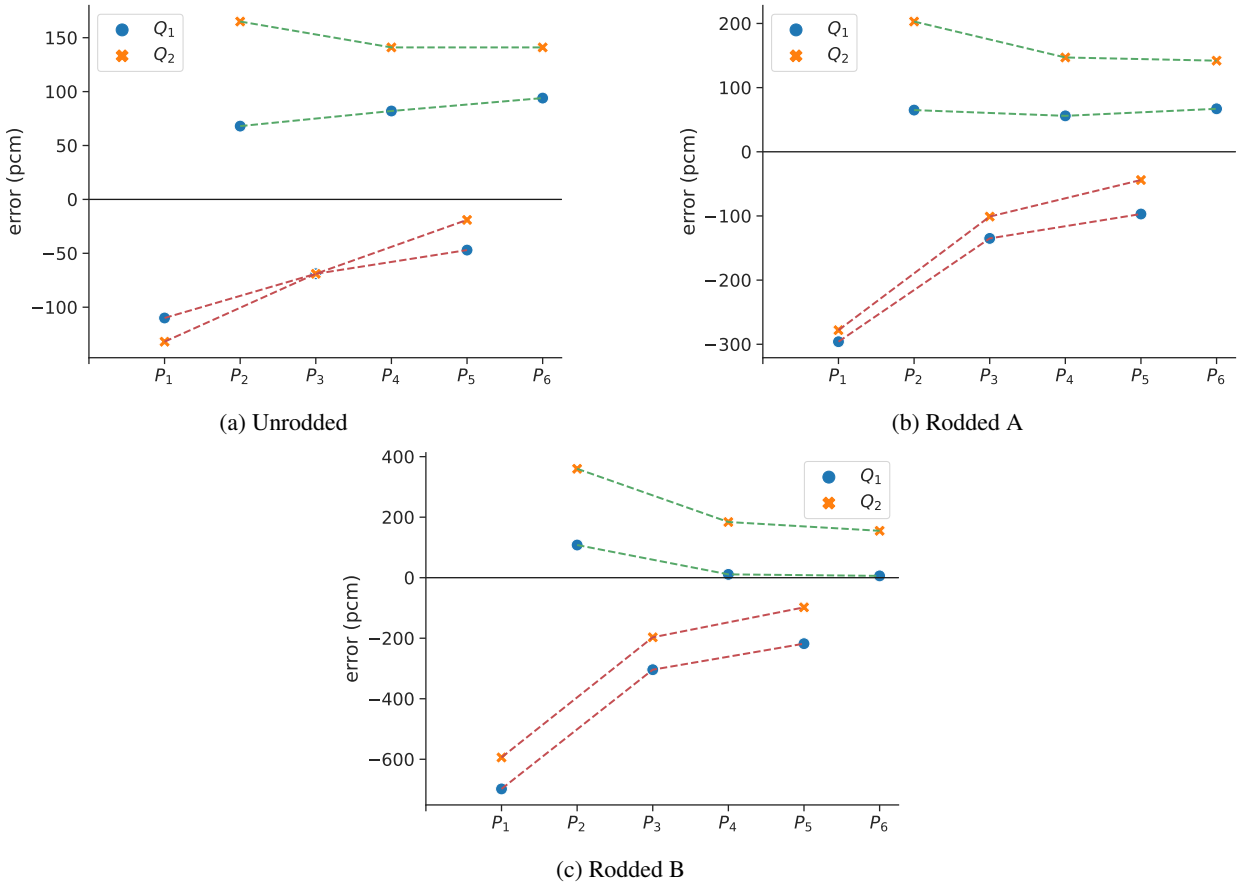

(a) Unrodded

(b) Rodded A

(c) Rodded B

Figure 5: Evolution of eigenvalue relative error (in pcm) according to the angular-space discretization for C5G7. Even (resp. odd) P_N orders are connected by green (resp. red) dotted line.

mean relative (MRE) errors on the pin power distribution (defined in [7, p. 25]). For the first two cases, the calculations exhibit errors less than 0.6% compared to the MCNP solution. We obtain a slightly bigger error (less than 1%) on the last case because of strong discontinuities introduced by control rods insertion. In overall, these results comply well with the reference values.

Table 2: Eigenvalue error and pin power distribution metrics for C5G7 benchmark problem. Calculations are done with $P_5\ Q_2\ Z_1$ for the first two cases and $P_6\ Q_1\ Z_2$ for Rodded B.

Benchmark case		Unrodded	Rodded A	Rodded B
Eigenvalue error (pcm)		12	-29	6
Pin power error (%)	Max Rate	-0.084	-0.398	-1.221
	AVG	0.225	0.301	0.743
	RMS	0.280	0.398	0.835
	MRE	0.171	0.249	0.764
Assembly power error (%)	UOx Inner	0.014	-0.178	-0.980
	MOx	-0.135	0.041	0.476
	UOx Outer	0.365	0.662	0.866
Cpu time (s)		5191	5389	6084

4 Conclusions

The implementation of the three-dimensional extension of the previously developed discontinuous Galerkin P_N method has been described and its capabilities illustrated on the examples of the well-known Takeda and C5G7 benchmarks. The discretisation method is able to handle the mesh elements of different shape, in general arbitrary, but in practical applications all geometries describing the fuel elements without any simplification nor homogenisation. The presented results show that the method is able to attain the accuracy better than 100 pcm in reactivity for a computation time less than 10 minutes on a desktop machine. The investigated cases show the error smaller than 30 pcm and in some of these of order of one pcm.

The convergence behaviour of odd and even order expansions are different and need further theoretical analysis. Nevertheless, the method seems to be consistent and stable showing competitive computational times, such that opens the possibilities to consider the problems in high fidelity having a whole core size. Evidently, this approach needs the implementation of a distributed memory parallel algorithm.

In this work, we presented the well-known few-group benchmarks that all defined with isotropic scattering, though the solver takes in charge anisotropic scattering expansion to an arbitrary order. The tests that are out of scope of this paper have been conducted on the examples of PWR assemblies in 281 energy groups with different scattering orders, and the obtained results agreed well with other, characteristic-based transport solvers.

Future analysis will also comprise the comparison with other 3D transport solvers, mainly method of characteristics of APOLLO3® [11].

ACKNOWLEDGEMENTS

K. Assogba's PhD research work is supported by the CEA NUMERICS program, which has received funding from the European Union's Horizon 2020 research and innovation program under the Marie Sklodowska-Curie grant agreement No 800945.

REFERENCES

[1] L. Bourhrara. "New Variational Formulations for the Neutron Transport Equation". en. In: *Transport Theory and Statistical Physics* 33.2 (Jan. 2004), pp. 93–124. DOI: 10.1081/TT-120037803.

[2] L. Bourhrara. "A new numerical method for solving the Boltzmann transport equation using the PN method and the discontinuous finite elements on unstructured and curved meshes". In: *Journal of Computational Physics* 397 (July 2019). DOI: 10.1016/j.jcp.2019.07.001.

[3] S. Keller and C. Oliveira. "Two-dimensional C5G7 mox fuel assembly benchmark calculations using the FEM-PN code EVENT". In: *Progress in Nuclear Energy* 45 (2004), pp. 255–263.

[4] M. A. Smith, E. E. Lewis, and E. R. Shemon. "DIF3D-VARIANT 11.0: A Decade of Updates". In: (Apr. 2014). DOI: 10.2172/1127298.

[5] D. Schneider et al. "APOLLO3® CEA/DEN deterministic multi-purpose code for reactor physics analysis". In: *PHYSOR 2016 – Unifying Theory and Experiments in the 21st Century*. Sun Valley, United States, May 2016.

[6] T. Takeda and H. Ikeda. "3-D Neutron Transport Benchmarks". In: *Journal of Nuclear Science and Technology* 28.7 (1991), pp. 656–669. DOI: 10.3327/jnst.28.656.

[7] E. E. Lewis et al. "Benchmark specifications for deterministic MOX fuel assembly transport calculations without spatial homogenization (3-D extension C5G7 MOX)". In: *OECD/NEA report* 6 (2003).

[8] T. M. MacRobert and I. N. Sneddon. *Spherical harmonics : an elementary treatise on harmonic functions, with applications, 3rd ed. rev*. Oxford, England: Pergamon press, 1967.

[9] A. Seubert, W. Zwermann, and S. Langenbuch. "Solution of the C5G7 3-D extension benchmark by the SN code TORT". en. In: *Progress in Nuclear Energy*. OECD/NEA C5G7 MOX Benchmark: 3-D Extension Case 48.5 (July 2006), pp. 432–438. DOI: 10.1016/j.pnucene.2006.01.007.

[10] S. Criekingen, E. Lewis, and R. Beauwens. "Mixed-Hybrid Transport Discretization Using Even and Odd PN Expansions". In: *Nuclear Science and Engineering* 152 (Feb. 2006). DOI: 10.13182/NSE06-1.

[11] A. Gammicchia, S. Santandrea, and S. Dulla. "Cross sections polynomial axial expansion within the APOLLO3® 3D characteristics method". In: *Annals of Nuclear Energy* 165 (2022), p. 108673.